

the previous one terminates, but simply illustrate the way in which the termination process of one event sets up the initiation environment for some future event.

The foregoing examples and the model suggest that bend zones are critical in earthquake mechanics and initiation and should be carefully monitored for precursory effects. The model suggests that, because bend zones by their nature involve faulting on a wide range of scales, earthquakes should also be monitored over a wide scale range if the physical processes in these regions are to be understood. Possibly, downhole seismometers should be used to detect tiny asperity-breaking events in the hypocentral region. The monitoring should not be too localized since activity prior to a main event can occur at a distance from the epicenter, forming a Mogi doughnut (34) (Fig. 5C).

It is evident that bends in faults are, in the long term, unstable features, and new fault geometries must inevitably result from continued tectonic motion. Nonetheless, repeated motion on fault segments does occur and produces clear morphological features from which the expected lifetime of a given segmentation geometry may be judged. One of the problems we face in characterizing the bend regions is also a geomorphological one. Although multiscale faulting may be expected to occur at depth, the faults will in general be too small to create surface breaks. We cannot expect the surface fault geometry to represent that at depth except for the grossest features. Individual small events do not generally form surface breaks, but repeated motion often results in the formation of near-surface warping, folding, and secondary faulting (5, 9, 35, 36). Identification of active horizontal drag-folds in the case of strike-slip faults and active anticlines or monoclines in the case of dip-slip faults is therefore important. It is also important to distinguish between secondary faulting that is a consequence of near-surface folding processes driven by fault motion at depth and surface faults that are the direct surface expression of seismic faulting at depth.

GEOFFREY KING

Department of Earth Sciences,
Bullard Laboratories,
Cambridge University,
Cambridge CB3 0EZ, England

JOHN NÁBĚLEK

Earth Resources Laboratory,
Department of Earth, Atmospheric,
and Planetary Sciences,
Massachusetts Institute of
Technology, Cambridge 02139

References and Notes

1. K. Aki, *J. Geophys. Res.* **84**, 6140 (1979).
2. S. Das and K. Aki, *ibid.* **82**, 5658 (1977).
3. A. G. Lindh and D. M. Boore, *Bull. Seismol. Soc. Am.* **71**, 95 (1981).
4. L. Sykes, *Predicting Great Earthquakes* (Lamont-Doherty Geological Observatory, Palisades, N.Y., 1983).
5. G. C. P. King and G. Yielding, *Geophys. J. R. Astron. Soc.* **77**, 915 (1984).
6. G. C. P. King, *Pure Appl. Geophys.* (Nos. 5 and 6) (1983).
7. W. Bakun and T. McEvelly, *J. Geophys. Res.* **89**, 3051 (1984).
8. M. I. Hussein *et al.*, *Geophys. J. R. Astron. Soc.* **43**, 367 (1975).
9. G. C. P. King and C. Vita-Finzi, *Nature (London)* **292**, 22 (1981).
10. G. C. P. King and J. Brewer, *ibid.* **306**, 147 (1983).
11. W. Bakun and A. Lindh, *Science*, in press.
12. H. L. Zhoua, C. Allen, H. Kanamori, *Bull. Seismol. Soc. Am.* **73**, 1585 (1983).
13. E. Arpart, *Yeryuvuri ve Insan* **2**, 15 (1977).
14. P. I. Yanev, *Earthquake Eng. Res. Inst.* (Ankara, Turkey) *Newsl.* (1975), vol. 9.
15. C. Soufferis, thesis, Cambridge University (1981).
16. M. Berberian, *Geophys. J. R. Astron. Soc.* **58**, 625 (1979).
17. J. Nábělek, thesis, Massachusetts Institute of Technology (1984).
18. State Seismological Bureau, Research Division, Preface of *Observation and Investigation of Tangshan Earthquake* (in Chinese) (Seismology Publisher, Peking, 1981), vol. 1.
19. J. Nábělek, W. P. Chen, H. Ye, in preparation.
20. M. N. Toksöz, E. Arpart, F. Saroglu, *Nature (London)* **270**, 423 (1977).
21. M. N. Toksöz, J. Nábělek, E. Arpart, *Tectonophysics* **49**, 199 (1978).
22. K. Kudo, in *A Comprehensive Study on Earthquakes in View of Seismic Risk Deduction*, Y. Ohta, Ed. (Hokkaido University, Sapporo, Japan, 1983), pp. 23-67.
23. J. Nábělek and M. N. Toksöz, internal report (Earth Resources Laboratory, Massachusetts Institute of Technology, Cambridge, 1984).
24. P. Reasenber and W. L. Ellsworth, *J. Geophys. Res.* **87**, 637 (1982).
25. M. Ouyed *et al.*, *Geophys. J. R. Astron. Soc.* **73**, 605 (1983).
26. A. Deschamps, Y. Gaudemer, A. Cisternas, *Bull. Seismol. Soc. Am.* **72**, 1111 (1982).
27. J. Nábělek, in preparation.
28. W. H. Bakun *et al.*, *Science* **225**, 288 (1984).
29. H. Kanamori, *U.S. Geol. Surv. Open-File Rep.* **78-380** (1978).
30. F. P. Bowden and D. Tabor, *The Friction and Lubrication of Solids* (Clarendon, London, 1964).
31. R. Madariaga, *Geophys. J. R. Astron. Soc.* **51**, 625 (1977).
32. S. Das, personal communication.
33. F. R. N. Nabarro, *Theory of Crystal Dislocations* (Oxford Univ. Press, Oxford, 1967), p. 21.
34. K. Mogi, in *Earthquake Prediction*, D. W. Simpson and P. G. Richards, Eds. (American Geophysical Union, Washington, D.C., 1981), pp. 635-666.
35. R. S. Stein and G. C. P. King, *Science* **224**, 869 (1984).
36. C. Vita-Finzi and G. C. P. King, *Proc. R. Soc. London*, in press.
37. We thank W. Bakun and A. Lindh for helpful discussions. Financial support for this work was provided by the Natural Environment Research Council (grant GR3/3904), the Royal Society of London, and U.S. Geological Survey (grant 14-08-0001-G-959). This is Cambridge Earth Science contribution No. 574.

21 September 1984; accepted 30 January 1985

A Model for a Seismic Computerized Alert Network

Abstract. *In large earthquakes, damaging ground motions may occur at large epicentral distances. Because of the relatively slow speed of seismic waves, it is possible to construct a system to provide short-term warning (as much as several tens of seconds) of imminent strong ground motions from major earthquakes. Automated safety responses could be triggered by users after receiving estimates of the arrival time and strength of shaking expected at an individual site. Although warning times are likely to be short for areas greatly damaged by relatively numerous earthquakes of moderate size, large areas that experience very strong shaking during great earthquakes would receive longer warning times.*

The purpose of a seismic computerized alert network (SCAN) is to provide short-term warning (as much as several tens of seconds) of imminent strong ground motion from large earthquakes. In earthquakes of great fault length, substantial damage often occurs at great distances from the earthquake's epicenter. It is possible to construct a system that would quickly detect strong ground motions in the epicentral area of major earthquakes. Information about the nature of an ongoing earthquake could then be transmitted to areas that may be strongly shaken when seismic energy propagates to them. This information could be processed automatically by individual users, and appropriate safeguard actions could be initiated.

The great earthquake of 1857 that ruptured a 300-km segment of the San Andreas fault in southern California is an example of how a SCAN could provide more than a minute of warning time

before the occurrence of strong shaking in a heavily populated area. There is evidence that the rupture initiated in the vicinity of Parkfield (1), a small town 275 km northwest of metropolitan Los Angeles. It seems likely that rupture propagated south toward the Los Angeles region at a velocity of about 3 km/sec or less, and the strongest shaking in the Los Angeles region probably occurred at least 100 seconds after the ground began to shake at Parkfield.

In similar earthquakes, a SCAN could provide users with information during this time so that they could initiate certain safety precautions. The most suitable applications are in those operations that come under computer control and can be safeguarded quickly. For example, a SCAN could initiate (i) electrical isolation and protection of delicate computer systems, (ii) isolation of electric power grids to avoid widespread blackouts, (iii) protection of hazardous chemi-

cal systems and offshore oil facilities, (iv) closing of natural gas valves to minimize fire hazards, (v) warning of nuclear power plants and national defense facilities, (vi) protection of emergency facilities such as hospitals and fire stations, and (vii) protection of fixed-rail transportation systems.

The basic features of a SCAN are schematically represented in Fig. 1. Ground motions recorded by a dense array of broadband, high dynamic-range seismometers are digitally telemetered to a central processing site. The occurrence of a large earthquake is detected and the location, time of origin, amplitude of ground shaking, and reliability estimates are transmitted instantly to microcomputers operated by individual users. The user's computer then combines this information with that about the user's site (for example, location and geologic conditions) to estimate the time of arrival and the nature of ground motions expected at the site. Decisions already programmed into the user's computer are then made on the basis of this information and the appropriate action is taken.

The problem of false alarms is minimized by continuous updates regarding the size of the ground motions at differing stations in the seismometer array. If a user is close to the epicenter of a developing earthquake, then the user's processor will recognize that little time is available to receive further information and immediate action may be necessary.

However, if the user is far from the epicenter, then considerable time is available before shaking begins. This time may be used to receive further information about the size of the earthquake. In this way, users at large epicentral distances take action only for the large earthquakes that present a real hazard, and each user adjusts the decision-making process to the needs of the site.

After the occurrence of a large earthquake, the seismometer array immediately provides information regarding the strength of shaking in different geographic locations. This information can be used to estimate regions of substantial damage, so that emergency services can be allocated promptly and properly. Because the seismometers in the array would have a large dynamic range, the SCAN may routinely record ground motions from numerous small earthquakes and teleseisms. Such data are important for basic research in the fields of ground-motion prediction, earthquake prediction, and earth structure. Also, the routine use of a SCAN for studies of numerous small events would help to ensure that the system operates properly when relatively rare large events occur.

The great earthquake of 1906 in San Francisco was in many ways similar to the 1857 event. However, there is evidence that its epicenter was close to metropolitan San Francisco (2), and thus little warning could have been given to the city. The damage caused by the

earthquakes at Long Beach in 1933 (magnitude, $6\frac{1}{4}$ on the Richter scale) and at San Fernando in 1971 (magnitude, $6\frac{1}{2}$) was more local with respect to the epicenters than that from the great San Andreas earthquakes, and again the warning times to the heavily damaged areas would have been short. Further, earthquakes of moderate size are more numerous than the major events, even though the area of intense shaking is smaller. To determine the probability that a SCAN user will receive a certain warning time for a certain degree of shaking, I used a simple mathematical model to compute the distributions of warning times for different levels of ground motion and for a set of earthquakes having different magnitudes.

In this model, an earthquake is approximated by rupture along a line source of length L extending along the surface of the earth. The energy magnitude M_w of the earthquake is determined from the rupture length by Eqs. 1 and 2.

$$M_w = 2 \log L + 4, M_w < 7.2 \quad (1)$$

$$M_w = 2/3 \log L + 6.1, M_w > 7.2 \quad (2)$$

where L is in kilometers. These equations were derived from theoretical relations between earthquake moment and rupture dimensions (3) for an average stress drop of 30 bars and a maximum fault width of 20 km.

The amplitude of ground shaking from this earthquake is described by Eq. 3 or 4.

$$\log \ddot{U} = -1.02 + 0.249M_w - 1/2 \log (R^2 + 21.1) - 0.00255 (R^2 + 21.1)^{1/2} \quad (3)$$

$$\log \dot{U} = 2.41 + 0.66 (M_w - 6) - 0.16 (M_w - 6)^2 - 1/2 \log (R^2 + 19.4) - 0.00429 (R^2 + 19.4)^{1/2} \quad (4)$$

where \ddot{U} is peak ground acceleration in units of gravitational acceleration, g (4), \dot{U} is response spectral velocity in centimeters per second for a 5 percent damped oscillator with a 1-second period (5), and R is the smallest horizontal distance in kilometers between an observer and the rupture. The geometry of the area receiving peak accelerations between \ddot{U} and $\ddot{U} + \Delta\ddot{U}$ is shown in Fig. 2. Equations 1 through 4 specify the ground motions everywhere about the hypothetical earthquake.

Warning times (T) for this earthquake are defined as the interval between the time of origin of the rupture and the arrival of direct S waves from the rupture at the point on the fault that is closest to the observer. The model is

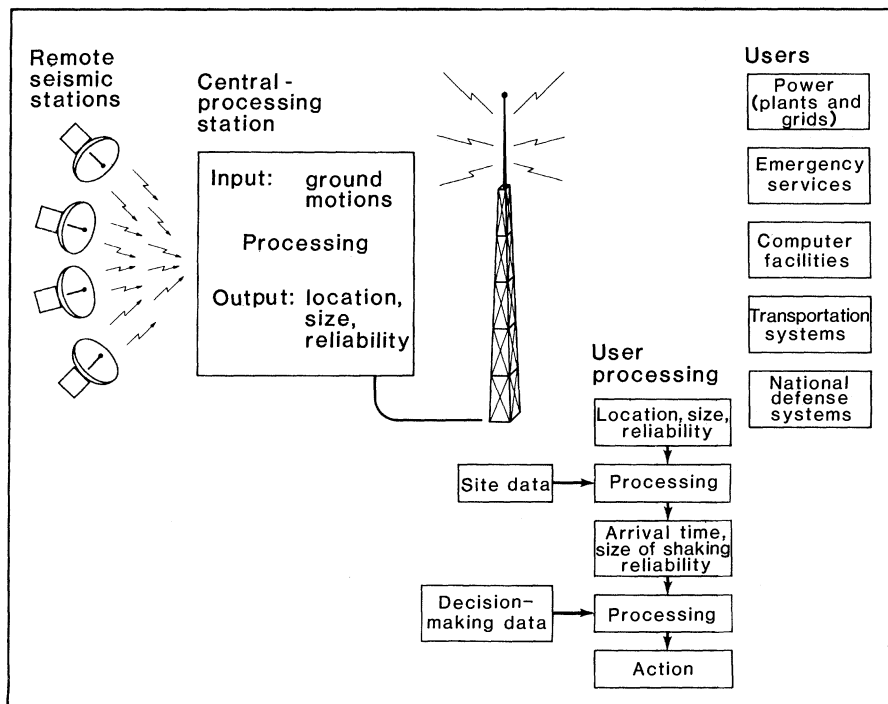


Fig. 1. Conceptual design of a seismic computerized alert network (SCAN).

based on unilateral rupture propagation at a velocity of 2.5 km/sec and an average shear-wave velocity of 3.5 km/sec. The warning times are given by Eqs. 5, 6, and 7, and their spatial distribution is shown in Fig. 2.

$$T = \frac{(x^2 + y^2)^{1/2}}{3.5}; x \leq 0 \quad (5)$$

$$T = \frac{x}{2.5} + \frac{|y|}{3.5}; 0 < x \leq L \quad (6)$$

$$T = \frac{L}{2.5} + \frac{[(x - L)^2 + y^2]^{1/2}}{3.5}; x > L \quad (7)$$

where x and y are distances from the epicenter. The amplitude of maximum shaking and its warning time are computed for every point within a specified distance of the fault.

The earthquake history of a region is incorporated by considering a collection of earthquakes having a specified frequency-magnitude distribution. The number of earthquakes N per 100 years between energy magnitudes $M_w - 0.05$ and $M_w + 0.05$ for southern California is approximated by Eq. 8 (6).

$$\log N = 6.89 - M_w \quad (8)$$

The model represents a set of earthquakes that obey Eq. 8 and that have magnitudes greater than 5.5 and less than 7.9 (rupture length of 380 km). The amounts of area receiving particular degrees of ground motion and warning time are computed for each earthquake in the set, and the results from all earthquakes are combined to give the overall distribution of area as a function of warning time and ground motion. The distribution of warning time as a function of peak acceleration is shown in Fig. 3. The contours give the probability that a user will receive at least a certain warning time in the event of at least a certain value of acceleration. The total area expected to receive that value of acceleration or greater during a 100-year period (see Fig. 3) may exceed the total area of southern California, which is about $3 \times 10^5 \text{ km}^2$, because many areas will experience low values of acceleration several times in a 100-year period.

The expected warning time is long at both low ($<0.1g$) and high ($>0.3g$) values of acceleration, but the expected warning time is short for moderate (0.1g to 0.3g) values. Because low accelerations occur at large distances between site and fault, the warning time is large for small accelerations. In this model, accelerations of 0.2g are most likely to occur close to the numerous moderate-sized earthquakes, and hence the expected warning time is short. Equation 4

implies that large accelerations result only from large earthquakes that have large rupture lengths. Thus areas that receive large accelerations can also expect to receive large warning times.

Although relatively large peak accelerations occur at small distances from the numerous smaller earthquakes, they rarely cause great damage because the duration of intense shaking is short. Response spectral velocities of 1 second are usually considered to give a better estimate of damage potential than peak acceleration. The distribution of warning time as a function of response spectral velocity is shown in Fig. 4 for the model described above. The same general features for peak acceleration are seen for response spectral velocity. However, the probability of receiving warning times of less than 10 seconds for potentially damaging motions is less than that indicated by modeling peak acceleration. In this model, substantial response spectral velocities are only produced by major earthquakes of large rupture lengths.

Warning times given in the model are based on the assumption that an earth-

quake is detected instantaneously. However, there is some delay because the first reporting seismometer will probably be at an appreciable distance from the epicenter for an array with a reasonable number of seismometers. The number of seismometers necessary to keep this delay at an acceptable level varies with the expected geometric distribution of earthquakes. If the earthquakes are assumed to occur along a small number of known faults of total length L , then a SCAN might consist of n stations evenly distributed along those faults. If hypocentral depths are assumed to be negligible, then the mean travel time \bar{T} of the P waves from a uniform random distribution of epicenters on the fault to the closest station is

$$\bar{T} = \frac{L}{4Cn} \quad (9)$$

where C is the velocity of the P waves. If L is 10^3 km , and if there are 50 seismometers, then the mean P wave travel time to the closest station is 0.83 second.

If the earthquakes are assumed to be randomly distributed throughout an area

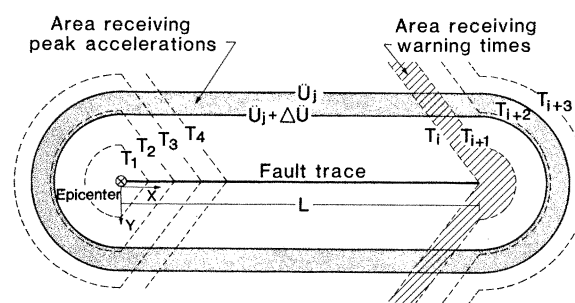


Fig. 2. Diagram of model used to compute the area that receives a warning time between T_i and T_{i+1} and that also experiences a peak acceleration between U_j and $U_j + \Delta U$. Warning times and peak accelerations are computed for every point within a specified distance of the fault. Results are then combined for an ensemble of earthquakes having differing rupture lengths L .

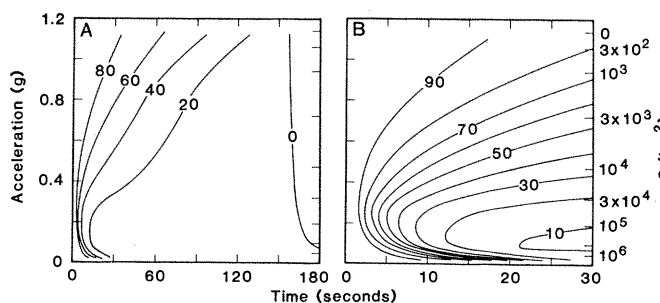


Fig. 3. Distribution of warning times as a function of the expected peak acceleration. Contours denote percent of area having a peak acceleration of U or greater that receive a warning time of T or greater. S is the total area to receive a peak acceleration of U or greater in a 100-year period in southern California. Warning time is given relative to the arrival time of maximum shaking. (B) is the same as (A) but with an expanded time scale.

a 100-year period in southern California. Warning time is given relative to the arrival time of maximum shaking. (B) is the same as (A) but with an expanded time scale.

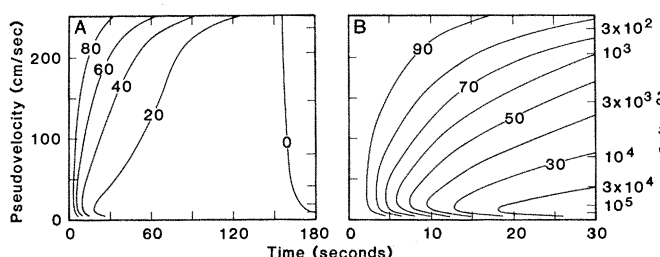


Fig. 4. Distribution of warning times as a function of the expected response spectral velocity. (B) is the same as (A) but with an expanded time scale.

A, then a SCAN might consist of n stations that are evenly distributed over that area. If hypocentral depths are assumed to be negligible, then the mean P wave travel time \bar{T} from a uniform random distribution of epicenters to the closest station is

$$\bar{T} = \frac{0.3825}{C} \sqrt{\frac{A}{N}} \quad (10)$$

If we assume an area of 3×10^5 km², 500 seismometers, and a P wave velocity of 6 km/sec, the mean P wave travel time to the closest station is 1.56 seconds.

The model just presented is a very simple one. Ground motions are considered to be a simple function of distance and magnitude. However, the standard deviation of data on ground motions for actual earthquakes with respect to these functions is typically of the order of 50 percent. Furthermore, little or no data exist for sites at small distances from large earthquakes, and the predicted ground motions for such situations vary greatly with the technique used to extrapolate these functions into a region of sparse data. Other simplifications were made in the computation of warning times. For example, the model does not include the effect of the finite depth of hypocenters, nor does it account for the distance between the first reporting seismometer and the epicenter. Also, a delay is introduced by data processing and telemetry. If these effects are included, then it is likely that the warning times shown in Figs. 3 and 4 would be reduced by several seconds. Because shaking from the initial P wave may be weak, particularly if the epicenter is at a great distance, warning times in Figs. 3 and 4 are given for the S wave from the closest point on the rupture. However, in many instances appreciable shaking may occur before this time, and the exact definition of warning time becomes uncertain. If the warning times in Figs. 3 and 4 are computed for the arrival time of hypocentral P waves instead of S waves from the closest point on the rupture, then warning times are decreased by about a factor of 2.

Southern California is only one of the regions that might benefit from a SCAN. Large subduction earthquakes are a threat to much of the circum-Pacific region, and evidence suggests that they might constitute a threat in the northwestern United States (7). Great shallow earthquakes in subduction zones sometimes have very long rupture lengths. For instance, the rupture length of the 1964 Alaskan earthquake probably exceeded 400 km. Because of the potential for large rupture dimensions, a SCAN

could provide substantial warning times for shallow subduction earthquakes.

Intraplate earthquakes, such as the New Madrid earthquakes in 1811 and 1812 or the 1886 Charleston earthquake, also constitute a threat. Although the mechanisms of these earthquakes are poorly understood, these events probably do not involve large rupture dimensions (8). Nevertheless, the felt areas of these earthquakes were larger than those for the largest of the California earthquakes (9). It is generally thought that the principal reason for this phenomenon is a lesser degree of attenuation of seismic waves east of the Rocky Mountains. Because rupture lengths of great earthquakes in the central and eastern United States may be less than 50 km, the regions of strongest shaking that lie adjacent to the rupture zone are not likely to receive large warning times. However, other models (7) indicate that Rossi-Forel intensities of IX and VIII may have extended to epicentral distances of 100 and 200 km, respectively, for the

1811 to 1812 New Madrid earthquakes. This means that a SCAN could still provide large warning times for areas shaken strongly enough to cause great damage.

THOMAS H. HEATON
U.S. Geological Survey, Seismological
Laboratory, California Institute
of Technology, Pasadena 91125

References and Notes

1. K. E. Sieh, *Bull. Seism. Soc. Am.* **68**, 1731 (1978).
2. D. M. Boore, *ibid.* **67**, 561 (1977).
3. T. H. Heaton, F. Tajima, A. W. Mori, unpublished data.
4. W. B. Joyner and D. M. Boore, *Bull. Seism. Soc. Am.* **71**, 2011 (1981).
5. _____, *U.S. Geol. Surv. Open-File Rep.* 82-977 (1982).
6. J. A. Hileman, thesis, California Institute of Technology, Pasadena (1977).
7. T. H. Heaton and H. Kanamori, *Bull. Seism. Soc. Am.* **74**, 933 (1984).
8. J. F. Evernden, W. M. Kohler, G. D. Clow, *U.S. Geol. Surv. Prof. Pap.* 1223 (1981).
9. O. W. Nuttli and J. E. Zollweg, *Bull. Seism. Soc. Am.* **64**, 73 (1974).
10. I thank W. Gates and W. Iwan for helpful discussion and for originally suggesting this topic to me and R. Page and J. Dieterich for review of the manuscript.

27 November 1984; accepted 27 February 1985

Adherent Bacterial Colonization in the Pathogenesis of Osteomyelitis

Abstract. *Direct scanning electron microscopy of material obtained during surgical debridement of osteomyelitic bone showed that the infecting bacteria grew in coherent microcolonies in an adherent biofilm so extensive it often obscured the infected bone surfaces. Transmission electron microscopy showed this biofilm to have a fibrous matrix, to contain some host cells, and to contain many bacteria around which matrix fibers were often concentrated. Many bacterial morphotypes were present in these biofilms, and each bacterium was surrounded by exopolysaccharide polymers, which are known to mediate formation of microcolonies and adhesion of bacteria to surfaces in natural ecosystems and in infections related to biomaterials. The adherent mode of growth may reduce the susceptibility of these organisms to host clearance mechanisms and antibiotic therapy and thus may be a fundamental factor in acute and chronic osteomyelitis.*

Adherence of bacteria in extensive microcolonies appears to be a fundamental step in the development of certain infectious disease states (1). Adherence may be mediated by highly hydrated, anionic exopolysaccharide polymers of the infecting bacteria which bind to the teichoic acid polymers of the Gram-positive cell wall (2, 3) and to the distal portions of the lipopolysaccharides of the Gram-negative cell wall (2). They often surround the bacterial cell in a fibrous matrix 0.5 to 1.0 μ m thick.

Adherent bacteria have been demonstrated on compromised bone, infected orthopedic prostheses and methyl methacrylate, and tissues adjacent to those foreign substances (4-7). Such infections tend to resist treatment and to persist until the biomaterial and the infected

adjacent tissue are removed (4-8); they are sometimes polymicrobial (8-10), and the adherent bacteria are difficult to detect unless special recovery and culture techniques are used (4, 9, 10). The natural mode of growth of many adherent bacteria in nature and in some diseases is polymicrobial, involving symbiotic mixed forms of aerobes and anaerobes (2, 4, 11, 12) coexisting in a biofilm held together by a ruthenium red-staining matrix (13). These structured biofilms occasionally shed bacteria into the ambient milieu or, in an infection, into the adjacent tissue fluids and circulatory system (4-7). The shed bacteria are not necessarily representative of the adherent colonies, but they are the bacteria that are recovered by conventional sampling techniques.